TSINGHUA SCIENCE AND TECHNOLOGY
ISSN 1007-0214 11/25 pp636-643
Volume 13, Number 5, October 2008

Longitudinal Acceleration Tracking Control of Low Speed Heavy-Duty Vehicles

WANG Yuejian (王跃建), BIN Yang (宾 洋), LI Keqiang (李克强)**

State Key Laboratory of Automotive Safety and Energy, Department of Automotive Engineering, Tsinghua University, Beijing 100084, China

Abstract: This paper presents a model matching control (MMC) method based on the sliding mode control (SMC) method for longitudinal acceleration tracking control in a vehicular stop-and-go cruise control system. The nonlinearity of the vehicle acceleration response at low speeds was analyzed to develop a transfer function model of the vehicle longitudinal dynamics using the least-mean-square system identification technique. This transfer function was then used to design the MMC controller, including an SMC feedback compensator. The system combines the advantages of the two control methods with robust control and rapid response. Simulations show that the controller enhances the rapid trackability to the vehicle acceleration and improves the system's robustness at low speeds compared with conventional PID MMC controllers.

Key words: stop-and-go cruise control system; nonlinearity; model matching control; sliding mode control

Introduction

The automotive industry has been encouraging the development of advanced concepts that may lead to more efficient traffic flow[1]. To successfully cope with low-speed travel in heavy traffic, adaptive control is needed in an advanced cruise control system for stop-and-go cruise control. The goal of stop-and-go cruise control is to assist human drivers in heavy traffic by reducing the need to frequently accelerate/decelerate at the low speeds.

Stop-and-go cruise control systems must be based on empirical studies of naturalist driving habits with measurements, data processing, model evaluation, and model-based analyses[2-4]. In general, adaptive cruise control systems operate at vehicle velocities of more than 30 km/h with large headways (i.e. the safe distance between vehicles). For stop-and-go cruise control systems, however, the vehicle is always operating on busy urban roads, with the velocity and headway reduced significantly in a complex environment. Since the dynamic characteristics of the engine, torque converter, and throttle/brake actuator are quite complex at low speeds, the lower layer control system must take into account the nonlinearities of the vehicle longitudinal dynamics[5].

Several methods have been used to design lower layer controllers. A conventional PID controller was used by Yi et al.[6,7] to control the dynamic characteristics of the engine and the torque converter. Yamamura et al.[8] used the model matching control (MMC) method based on a PID feedback compensator to design the lower layer controller to obtain improved rapid response compared with the traditional PID method. Venhovens et al.[2] proposed a synthesis control method to realize stop-and-go cruise control with more robust performance based on feedback of the acceleration error. However, in all these controllers, the feedback compensators were designed based on fixed linear systems, so the controllers cannot provide robust control and rapid response. Therefore, satisfactory acceleration tracking control is difficulty to realize in the

Received: 2007-06-10

** To whom correspondence should be addressed.
E-mail: likq@tsinghua.edu.cn; Tel: 86-10-62788774

stop-and-go control system because the systems do not consider the nonlinearities and parameter perturbations of the system at low speeds.

This study investigates the nonlinearities of the acceleration response of a heavy-duty vehicle at low speeds to design a nominal transfer function model of the dynamic system using the least-mean-square (LMS) system identification technique. The nominal transfer function model is then used to design an MMC controller including a sliding mode control (SMC) feedback compensator which combines robust control and rapid response. Simulations show that the controller enhances the rapid trackability to vehicle acceleration and improves the system's robustness in stop-and-go operation.

1 Analysis of System Acceleration Response Characteristics

1.1 Heavy-duty vehicle model

The simulation model for the longitudinal dynamics was developed using dynamics. The model consists of the car body, wheels, engine, torque convertor, and automatic transmission as shown in Fig. 1.

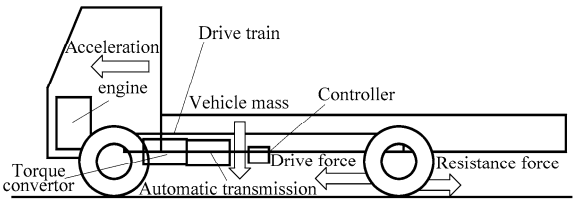

Fig. 1 Heavy-duty vehicle model

For the power train, the engine torque, te, is a nonlinear function of the engine speed, re, and the throttle angle, (°). The torque convertor is a nonlinear function of the capacity factor and the torque ratio as shown in Fig. 2.

The resistance force results from the influence of air drag, fa, rolling drag, fr, and climbing drag, fc.

These nonlinear effects were included in a simulation to verify the accuracy of the heavy-duty vehicle model and to get the steady-state longitudinal acceleration operating characteristics for various throttle angles and velocities as shown in Fig. 3 where % is the percentage of throttle angles.

The results show that the dynamics are quite nonlinear at low speeds (i.e. less than 10 m/s) compared with the good linearity at high speeds (larger than 10 m/s). Therefore, the acceleration response at low speeds must be analyzed for heavy-duty vehicles.

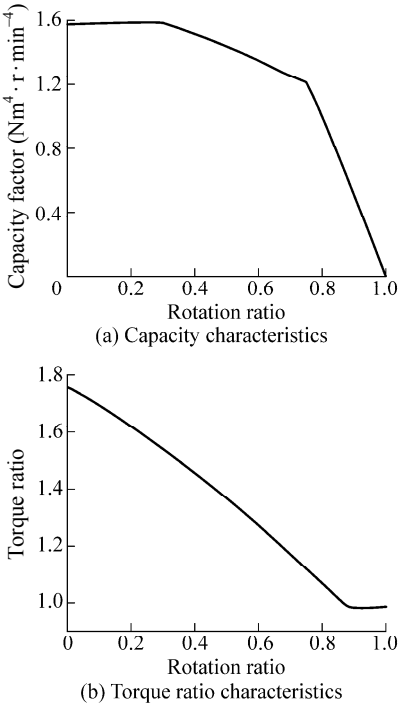

Fig. 2 Torque convertor characteristics

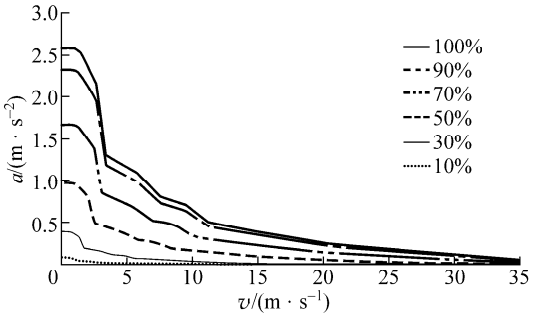

Fig. 3 Longitudinal acceleration dynamics for weight of 16 000 kg

1.2 Lower layer control system

The lower layer control system is shown as Fig. 4, where Throt is the throttle angle, Acc Tgt is the target acceleration, EBS is the electronic brake system. It includes the vehicle model and its inverse model.

Since this paper only concentrates on the acceleration tracking problem, the brake system control is omitted. The control system works by having the lower layer controller first determine the target acceleration based on the desired acceleration given by the upper layer controller and the actual acceleration. Second, the inverse vehicle model calculates the throttle angle based on the target acceleration and current vehicle velocity. Finally, the throttle actuator realizes the throttle angle to make the actual vehicle acceleration achieve the desired acceleration.

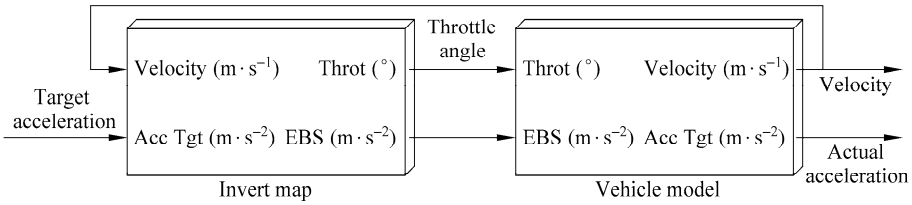

Fig. 4 Block diagram of lower layer system

1.3 Nonlinearities of the system acceleration response

The lower layer system's acceleration response characteristics and the factors that influence those characteristics at low speeds were analyzed for three test scenarios for different initial velocity, v_0, initial acceleration, a_0, and amplitudes of the input acceleration step, a_{rag}, (i.e. the error between the initial and final input step accelerations). The influence of these three factors on the system's acceleration response was investigated for a flat, straight road (road slope=0°) and a constant mass vehicle (m=20 000 kg). The frequency domain responses predicted by the simulations for various cases are shown in Figs. 5-7.

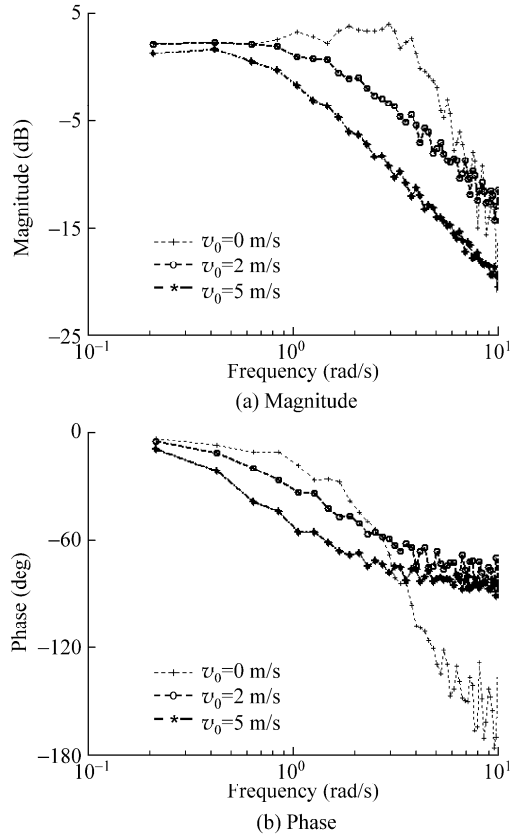

Fig. 5 Influence of initial velocity on the acceleration response for a_0=0 m/s^2 and a_{rag}=0.5 m/s^2

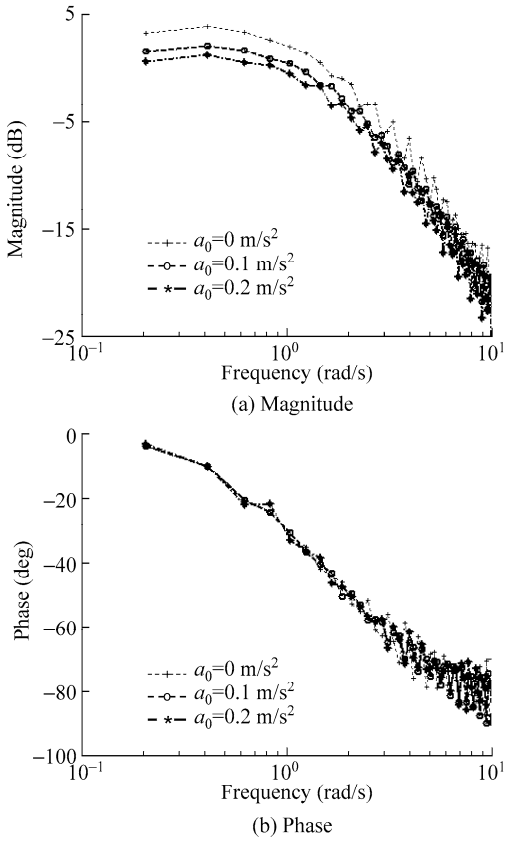

Fig. 6 Influence of a_0 on acceleration response for v_0=2 m/s and a_{rag}=0.3 m/s^2

Figure 5 shows that the magnitude and phase of the acceleration response are strongly influenced by v_0 with the response gradually changing from third order to second order as v_0 increases. Figure 6 shows that only the static magnitude is strongly influenced by a_0 at low frequencies, while a_0 has little effect with phase frequency. Figure 7 shows that both the magnitude and the phase of acceleration response are influenced by a_{rag}.

The acceleration response characteristics are summarized in Table 1, where a_p is the maximum percentage over-shoot, t_d is the delay time, s_{te} is the steady state error. These characteristics of the acceleration response change with the vehicle operating state (i.e. the initial velocity, initial acceleration, and input acceleration

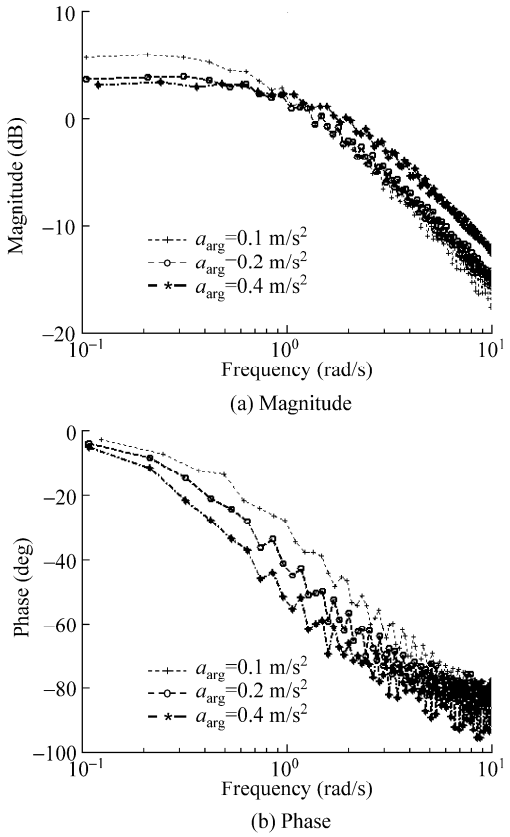

Fig. 7 Influence of a_{rag} on acceleration response for v_0=2 m/s and a_0=0.1 m/s^2

step amplitude) at low speeds. For Case 1, a_p decreased and t_d increased as v_0 increased while s_{te} was only slightly influenced by v_0. Case 2 shows that t_d and a_p both decreased as a_0 increased, while s_{te} increased. Case 3 shows that s_{te} increased and t_d decreased as a_{rag} increased, while a_p was only slightly influenced by a_{rag}. Thus, the lower layer control system must respond to the nonlinearity characteristics of the acceleration response, which are mainly due to the dynamic characteristics of the engine and the torque converter.

Table 1 Parameters for system response characteristics

Case	Initial condition			System response		
	v_0	a_0	a_{rag}	a_p	t_d	s_{te}
	m/s	m/s^2	m/s^2	%	s	m/s^2
1	0	–	–	7	0.30	0.18
	2	0	0.5	0	0.70	0.18
	5	–	–	0	1.90	0.18
2	–	0	–	4	0.65	0.10
	2	0.1	0.3	2	0.45	0.16
	–	0.2	–	1	0.35	0.20
3	–	0.1	0.1	0	0.60	0.10
	2	–	0.2	0	0.58	0.14
	–	–	0.4	0	0.48	0.20

Since the transfer function for the entire system which is needed for the controller design, also varies, the lower layer controller must consider the effect of the nonlinear acceleration response at low speeds.

2 SMC Model Matching Controller

For accurate tracking control of the acceleration response and to attenuate the affects of the system nonlinearities, the lower layer controller must provide the following characteristics:

(1) Rapid control response with small tracking control errors;

(2) Good robustness for all vehicle dynamics related to the system nonlinearities and variations of the system parameters such as vehicle mass and road slope.

An MMC controller design based on the SMC method was selected for the lower level controller.

2.1 MMC theory

The model matching controller is illustrated in Fig. 8 where a_d is the desired acceleration, a_r is the reference acceleration, u_{FF} is the feed-forward control, u_{FB} is the feedback control, u_{MMC} is the model matching control, $G_p(s)$ is the system transfer function, $G_m(s)$ is the reference transfer function, and C is the feedback compensator.

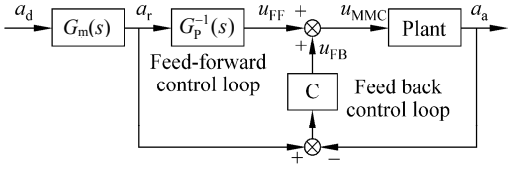

Fig. 8 Block diagram of model matching control

The model matching control system includes two loops.

(1) The feed-forward control loop, $G_m(s)\cdot G_p^{-1}(s)$, improves the rapid control response and accounts for the driver's behavior by the phase compensator (i.e. the inverse system $G_p^{-1}(s)$) of the plant transfer function $G_p(s)$ and the transfer function $G_m(s)$ of the reference model.

(2) The feedback control loop, C, eliminates the tracking control error between the actual and reference accelerations.

In the MMC controller, the feedback compensator, C, has intensive influence on the control system

performance. Conventional feedback control loops use PID, H-infinity on the designs with the nonlinearities of the vehicle response at low speeds, and with the wide variation of the system parameters such as the vehicle mass and road slope, the PID method is unable to provide adequate control system performance. In addition, although the H-infinity method is more robust to the uncertainties in the system, the design cannot guarantee that the upper and lower bounds of the uncertainties are known. Therefore, the nonlinear SMC control method[9,10] was used for the feedback compensator C in the MMC controller to overcome the limitation of the conventional PID and H-infinity methods.

2.2 MMC controller design

The first step to design an MMC controller is to determine the system transfer function. Here, the transfer function was determined from the heavy-duty vehicle parameters and its dynamic system constructed using the Matlab/Simulink dynamic system analysis tool. The analysis shows that the system transfer function varies with the operating state including the initial conditions especially the initial velocity, and the system parameters (i.e. vehicle mass). The nominal transfer function was defined for a vehicle m=20 000 kg, road slope=0°, a_0=0 m/s^2, and u=0-0.5 m/s^2. The LMS system identification technique was used to identify the nominal transfer function as

$$G_{\mathrm{P}}(s)=\frac{a_{\mathrm{a}}}{u}=\frac{9}{s^2+3.6v_0s+9.1} \tag{1}$$

where u is the control signal input (i.e. acceleration) and a_{a} is the actual acceleration output. The simplified transfer function Eq. (1) is compared with simulation results in Fig. 9. The actual acceleration agrees reasonably well with the desired acceleration so the design can be used in the lower layer control system with the MMC method.

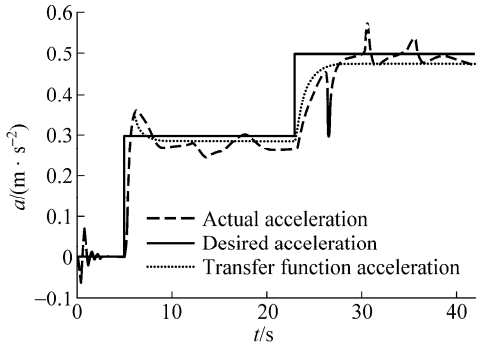

Fig. 9 Comparison of transfer function

Using inverse Laplace transformations, Eq. (1) can be formulated as the following differential equation:

$$9u=\ddot{a}_{\mathrm{a}}+3.6v_0\dot{a}_{\mathrm{a}}+9.1a_{\mathrm{a}} \tag{2}$$

Then, define the acceleration error as

$$\varepsilon=a_{\mathrm{r}}-a_{\mathrm{a}} \tag{3}$$

where $a_{\mathrm{r}}(s)=a_{\mathrm{d}}(s)\cdot G_{\mathrm{m}}(s)$ in which a_{r} is the reference acceleration and a_{a} is the desired acceleration.

Then, define a sliding surface as

$$S=\dot{\varepsilon}+a_{\mathrm{s}}\varepsilon+b_{\mathrm{s}}\int\varepsilon \tag{4}$$

where a_{s} and b_{s} are related parameters. The derivative of the sliding surface in Eq. (4) is

$$\dot{S}=(\ddot{a}_{\mathrm{r}}+a_{\mathrm{s}}\dot{a}_{\mathrm{r}}+b_{\mathrm{s}}a_{\mathrm{r}})-(\ddot{a}_{\mathrm{a}}+a_{\mathrm{s}}\dot{a}_{\mathrm{a}}+b_{\mathrm{s}}a_{\mathrm{a}}) \tag{5}$$

$$\dot{S}S<0 \tag{6}$$

Inequation (6) is the sufficient condition for the sliding mode to exist.

Substituting Eq. (2) into Eq. (5) yields

$$\dot{S}=(\ddot{a}_{\mathrm{r}}+a_{\mathrm{s}}\dot{a}_{\mathrm{r}}+b_{\mathrm{s}}a_{\mathrm{r}})-\left[9u+(a_{\mathrm{s}}-3.6v_0)\dot{a}_{\mathrm{a}}+(b_{\mathrm{s}}-9.1)a_{\mathrm{a}}\right]=-\eta\mathrm{sat}(S) \tag{7}$$

where η is the control parameter, sat(S) is the saturation function. To prevent oscillation of control result, sat (S) was chosen as

$$\mathrm{sat}(S)=\begin{cases}1, & S>\phi;\\ -1, & S<-\phi;\\ S/\phi, & \text{others}\end{cases} \tag{8}$$

From Eq. (7), the feedback control, u_{FB}, can be deduced as

$$u_{\mathrm{FB}}=u=\frac{(\ddot{a}_{\mathrm{r}}+a_{\mathrm{s}}\dot{a}_{\mathrm{r}}+b_{\mathrm{s}}a_{\mathrm{r}})-(a_{\mathrm{s}}-3.6v_0)\dot{a}_{\mathrm{a}}-(b_{\mathrm{s}}-9.1)a_{\mathrm{a}}+\eta\mathrm{sat}(S)}{9} \tag{9}$$

The feed-forward controller design is based on the transfer function in the reference model. Since the nominal system model was expressed as a second order transfer function, the reference transfer function needs to be at least second, so it can be defined as

$$G_{\mathrm{m}}(s)=\frac{\lambda}{s^2+\xi s+\lambda} \tag{10}$$

Considering the acceleration tracking behavior of the average driver during stop-and-go conditions, ξ and λ are assumed to be $\xi=5$ and $\lambda=10$ to guarantee adequate tracking accuracy and smooth driving performance. Then, the feed-forward control output is

$$u_{\mathrm{FF}}(s)=a_{\mathrm{d}}(s)G_{\mathrm{m}}(s)G_{\mathrm{P}}^{-1}(s) \tag{11}$$

The model matching control, u_{MMC}, is then

determined based on Eq. (12).

$$u_{\mathrm{MMC}} = u_{\mathrm{FB}} + u_{\mathrm{FF}} \tag{12}$$

2.3 Control system stability

For the variable structure control system, the stability is achieved by properly designing the sliding surface described in Eq. (4). Substitute Eq. (2) into Eq. (5) and let $\dot{S} = 0$, then the equivalent control is

$$u_{\mathrm{eq}} = \frac{(\ddot{a}_{\mathrm{r}} + a_{\mathrm{s}}\dot{a}_{\mathrm{r}} + b_{\mathrm{s}}a_{\mathrm{r}}) - (a_{\mathrm{s}} - 3.6v_0)\dot{a}_{\mathrm{a}} - (b_{\mathrm{s}} - 9.1)a_{\mathrm{a}}}{9} \tag{13}$$

Substituting the equivalent control into Eq. (2) yields

$$\ddot{\varepsilon} + a_{\mathrm{s}}\dot{\varepsilon} + b_{\mathrm{s}}\varepsilon = 0 \tag{14}$$

To satisfy global stability, a_{s} and b_{s} must be selected so that the eigenvalue of Eq. (14) is on the left side of the complex plane.

2.4 Control system robustness

The system transfer function varies due to nonlinearities and parameter variation at low speeds and due to variations of the reference acceleration. Therefore, the control system robustness must be evaluated.

As a typical case, the influence of mass variations on the transfer function is studied here. Simulation results for various masses of 16 000-25 000 kg are shown in Fig. 10.

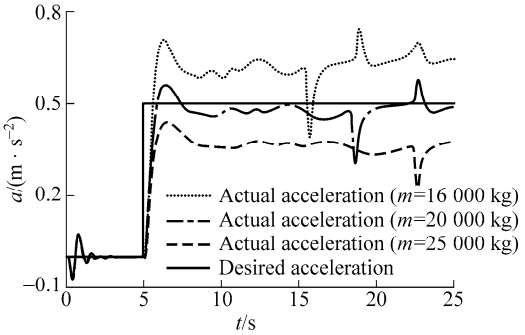

Fig. 10 Effect of mass variations on the acceleration response

Considering how the mass variations strongly influence the acceleration response, the actual transfer function $G_{\mathrm{p_a}}(s)$ can be defined as

$$G_{\mathrm{p_a}}(s) = \frac{a_a}{u} = \frac{\alpha}{s^2 + 3.6v_0 s + (\gamma + \Delta\gamma)} \tag{15}$$

where $\alpha = 9$, $\gamma = 9.1$, and $\Delta\gamma$ is the disturbance term resulting from vehicle mass variations. For a road slope of 0°, v_0=2 m/s, a_0=0 m/s^2, u=0-0.5 m/s^2, and masses of 16 000-25 000 kg, the disturbance term range obtained using the LMS system identification technique is $-2.1 \leqslant \Delta\gamma \leqslant 1.9$.

The feedback control, u_{FB}, can be reformulated as

$$u_{\mathrm{FB}} = u_{\mathrm{eq}} + \frac{\eta \mathrm{sat}(s)}{9} \tag{16}$$

The inverse Laplace transformation of Eq. (15) is

$$\alpha u = \ddot{a}_{\mathrm{a}} + 3.6v_0\dot{a}_{\mathrm{a}} + (\gamma + \Delta\gamma)a_{\mathrm{a}} \tag{17}$$

Substituting Eq. (13) into Eq. (17) yields

$$\ddot{\varepsilon} + a_{\mathrm{s}}\dot{\varepsilon} + (b_{\mathrm{s}} + \Delta\gamma)\varepsilon = \Delta\gamma a_{\mathrm{r}} \tag{18}$$

The Laplace transformation of Eq. (18) gives the transfer function for the control system robustness

$$\frac{\varepsilon(s)}{a_{\mathrm{r}}(s)} = \frac{\Delta\gamma}{s^2 + a_{\mathrm{s}}s + (b_{\mathrm{s}} + \Delta\gamma)} \tag{19}$$

The nonlinear term induced by the initial velocity, $3.6v_0$, is counteracted by the sliding surface in Eq. (18); therefore, the invariance of the sliding mode, ε, can be satisfied with respect to the influence of the nonlinearity.

The dynamic characteristics of the transfer function in Eq. (19) are influenced by the system eigenvalue and the effect of the mass variation can be minimized by properly selecting a_{s} and b_{s} to improve the robustness of the control system. Additionally, using the final value theorem for Eq. (19), the static error for the system response is

$$\lim_{s\to 0}\frac{\varepsilon(s)}{a_{\mathrm{r}}(s)} = \lim_{s\to 0}\frac{\Delta\gamma}{s^2 + a_{\mathrm{s}}s + (b_{\mathrm{s}} + \Delta\gamma)} = \frac{\Delta\gamma}{b_{\mathrm{s}} + \Delta\gamma}.$$

Thus, to minimize the static error, b_{s} should be much large than $\Delta\gamma$.

The transfer function in Eq. (19) is a low-pass filter for the variations of the reference acceleration, a_{r}; therefore, the influence of the sliding mode induced by those variations is weakened by increasing the damping which reduces the amplitude.

3 Simulation Results

The controller performance was simulated for v_0=0 m/s, a_0=0.0 m/s^2, and a_{rag}=0.1m/s^2 at 0 s; a_0=0.1 m/s^2 and a_{rag}=0.15 m/s^2 at 10 s; a_0=0.25 m/s^2 and a_{rag}=0.1 m/s^2 at 45 s. The mass was varied from 16 000-25 000 kg and the road slope was 0°. These parameters represent typical operating conditions for heavy-duty vehicles.

Thus, the test scenario can evaluate the control system with consideration of the system nonlinearities and parameter variations at low speeds. The performance of the MMC-based SMC controller is compared with the performance of a traditional PID and an MMC based PID in Figs. 11-14.

The control parameters for the PID compensator were $K_P = 2$, $K_I = 1.6$, and $K_D = 0$ which give the best PID control results. The parameters for the SMC compensator were $\phi = 50$, $\eta = 255$, $a = 2.2519$, and $b = 50$ based on the previous analysis.

3.1 Simulation results

Case 1 m=16 000 kg. This case represents a vehicle mass which is less than the mass assumed to design the controller, with the simulation results illustrated in Figs. 11 and 12.

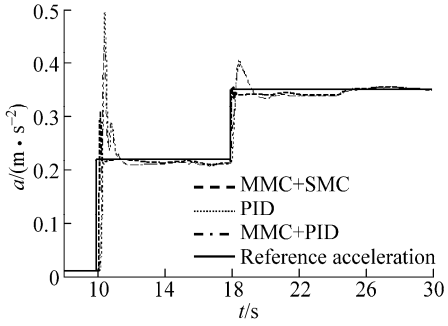

Fig. 11 Acceleration tracking curve for a vehicle mass less than the design mass

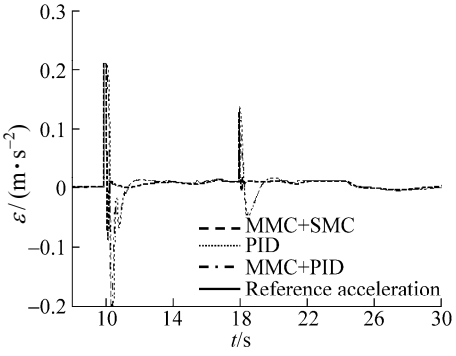

Fig. 12 Acceleration tracking error curve for a vehicle mass less than the design mass

Case 2 m=25 000 kg. This case represents a vehicle mass which is more than the mass used to design the controller, with the simulation results illustrated in Figs. 13 and 14.

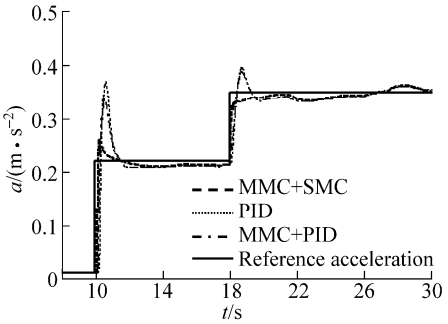

Fig. 13 Acceleration tracking curve for a vehicle mass more than the design mass

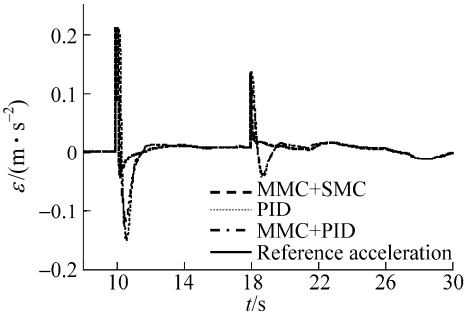

Fig. 14 Acceleration tracking error curve for a vehicle mass more than the design mass

3.2 Comparison analysis

Figures 11 and 13 show the accelerations for two vehicle weights less than and greater than the designed vehicle weight. Figures 12 and 14 show the acceleration tracking error curves. The maximum tracking error of the PID controller is ± 0.14 m/s^2 while that of the MMC-based PID is ± 0.1 m/s^2, with the PID exhibiting slower convergence. The maximum tracking error of the MMC-based SMC is almost zero even during the step response, and converges to the desired value faster without as much over-shoot.

Furthermore, the simulation results illustrate that the mass variation has a strong influence on the system's control performance. However, the tracking error of the MMC-based SMC controller is only slightly influenced by the mass variations even for the large change from 16 000 to 25 000 kg. Also, the MMC-based SMC controller is more robust than the other two controllers.

4 Conclusions

A longitudinal acceleration tracking control system was designed for a heavy-duty vehicle stop-and-go

cruise control system. The nonlinearities of the dynamic response during acceleration at low speeds were studied and the effects of the initial velocity, initial acceleration, and step amplitude of the input acceleration were identified. An MMC controller using the SMC feedback compensator was designed and evaluated for various vehicle masses. The advantages of the controller can be summarized as follows.

(1) The feed-forward loop of the matching control ensures that the controller responds rapidly as the actual acceleration converges to the desired value.

(2) The SMC feedback compensator in the MMC controller achieves better robustness to the system nonlinearities and parameter variations at low speeds.

Future research will improve the controller to attenuate spikes in the acceleration response resulting from gear switching.

References

[1] Marsden G, Mcdonald M, Brackstone M. Towards an understanding of adaptive cruise control. *Transportation Research Part C*, 2001, **9**(1): 33-51.

[2] Venhovens P, Naab K, Adiprasito B. Stop and go cruise control. In: Proc. FISITA World Automotive Congress. Seoul, 2000.

[3] Iljima T, Higashimata A, Tange S, et al. Development of an adaptive cruise control system with stop-and-go capability. SAE Paper, No. 2000-01-1353, 2000.

[4] Higashimata A, Adachi K, Hashizume T, et al. Design of a headway distance control system for ACC. *JSAE Review*, 2001, **22**(3): 15-22.

[5] Xu Z, Ioannou P. Adaptive throttle control for speed tracking. *Vehicle System Dynamics*, 1994, **23**: 293-306.

[6] Yi K, Moon I, Kwon Y D. A vehicle-to-vehicle distance control algorithm for stop and go cruise control. In: 2001 IEEE Intelligent Transportation Systems Conference Proceedings. Oakland, USA, 2001: 478-482.

[7] Yi K, Hong J, Kwon Y D. A vehicle control algorithm for stop-and-go cruise control. *Proc. Instn. Mech. Engrs.*, 2001, **215**(10): 1099-1115.

[8] Yamamura Y, Tabe M, Kanehira M, et al. Development of an adaptive cruise control system with stop and go capability. In: SAE 2001 World Congress. Detroit, Michigan, USA, 2001: 103-108.

[9] Hedrick J K. Nonlinear controller design for automated vehicle application. *IEE Conference Publication*, 1998, **455**(1): 23-32.

[10] Slotine J, Li W. Applied Nonlinear Control. Englewood Cliffs, New Jersey: Prentice-Hall, Inc., 1991.